PAPER • OPEN ACCESS

Electro collisions with molecular nitrogen in its ground and electronically excited states using the R-matrix method

View the article online for updates and enhancements.

Electro collisions with molecular nitrogen in its ground and electronically excited states using the R-matrix method

He Su[1] , Xinlu Cheng[2], Hong Zhang[1],* and **Jonathan Tennyson[3],***

[1] College of Physics, Sichuan University, Chengdu 610065, People's Republic of China
[2] Institute of Atomic and Molecular Physics, Sichuan University, Chengdu 610065, People's Republic of China
[3] Department of Physics and Astronomy, University College London, London, WC1E 6BT, United Kingdom

E-mail: hongzhang@scu.edu.cn and j.tennyson@ucl.ac.uk

Abstract

A comprehensive study of electron collisions with the $X\,^1\Sigma_g^+$ ground state as well as the metastable $A\,^3\Sigma_u^+$ and $a\,^1\Pi_g$ excited states of the N_2 molecule is reported using the fixed-nucleus R-matrix method. Integral elastic scattering and electronic excitation cross sections from the $X\,^1\Sigma_g^+$ ground state to the eight lowest electronic states, $A\,^3\Sigma_u^+$, $B\,^3\Pi_g$, $W\,^3\Delta_u$, $B'\,^3\Sigma_u^-$, $a\,^1\Pi_g$, $a'\,^1\Sigma_u^-$, $w\,^1\Delta_u$ and $C\,^3\Pi_u$, overall agree well with the available experimental and theoretical results although updates of some recommended values are suggested. Accurate electron impact electronic transition cross sections starting from the $A\,^3\Sigma_u^+$ and $a\,^1\Pi_g$ metastable excited states are reported. The total summed electronic transition cross sections from the $a\,^1\Pi_g$ state is dominant: an order of magnitude higher than those of the $X\,^1\Sigma_g^+$ ground state. The de-excitation cross sections generally show a downward trend with increasing incident electron energy, which is different from the elastic and electronic excitation cross sections which generally increase with collision energy. There is a prominent $^2\Pi_u$ symmetry resonance peak at 2.8 eV for electronic de-excitation scattering of $a^1\Pi_g \to B^3\Pi_g$, which significantly contributes to the total summed cross sections from the $a^1\Pi_g$ excited state. The present results provide a new insight which will aid understanding of electron spectra in the atmosphere of the Earth and Titan.

Keywords: electron collisions, electronic excitation, elastic scattering, cross sections, R-matrix method, nitrogen molecule

S Supplementary material for this article is available online

(Some figures may appear in colour only in the online journal)

* Authors to whom any correspondence should be addressed.

1. Introduction

Electron collisions with the nitrogen molecule are of particular importance in terrestrial and planetary atmospheres. They form the basis for understanding gaseous discharges, plasma processing, ionospheric and auroral phenomena as well as the other atmospheric and astronomical physical processes [1–6]. Among the scattering processes, molecular electronic excitation by electron impact is of particular interest. Excited molecules strongly affect reaction dynamics in plasma reactors because of their active nature; they also represent the main route for dissociation via multistep collision processes [7, 8]. For example, the metastable $A\ ^3\Sigma_u^+$ electronic excited state of N_2 can store energy for a long time so it is important in the elementary processes that control nitrogen discharges [9]. The excitation processes also play an important role in a number of prominent N_2 emissions. Notably the $a\ ^1\Pi_g$ electronic excited state undergoes transition to the $X\ ^1\Sigma_g^+$ ground state resulting in the ultraviolet (UV) emissions in the Lyman–Birge–Hopfield system [10, 11].

In order to properly account for the energy flow through the excited states of N_2 in plasma environments, accurate and reliable cross section data involving N_2 and electrons are required. In contrast to the situation for electronic transition processes involving N_2 excited states, a lot of work, both experimental and theoretical, has been performed on electron collisions with the N_2 ground state. Experimentally, Blaauw *et al* [12] and Muse *et al* [13] presented early reports of elastic electron scattering data; Malone *et al* [11, 14] and Campbell *et al* [15] extensively measured integral electronic excitation cross sections from ground state to the $A\ ^3\Sigma_u^+$, $B\ ^3\Pi_g$, $W\ ^3\Delta_u$, $B'\ ^3\Sigma_u^-$, $a\ ^1\Pi_g$, $a'\ ^1\Sigma_u^-$, $w\ ^1\Delta_u$, $C\ ^3\Pi_u$, $E\ ^3\Sigma_g^+$ and $a''\ ^1\Sigma_g^+$ states; subsequently Malone *et al* [16] added integral electronic excitation cross section data for another seven high-lying states of N_2. Considering measurements for specific electronic states, integral cross sections for electron impact excitation to the $a\ ^1\Pi_g$ state have been presented by several groups [10, 17, 18] who used different beam experiments. Zubek [19] measured total electronic excitation cross sections for the $C\ ^3\Pi_u$ state for incident electron energies from threshold to 17.5 eV, and recently Meng *et al* [20] used photoemission spectra to updated the $C\ ^3\Pi_u$ electronic excitation cross sections. Electronic excitation cross section to the higher $b\ ^1\Pi_u$ state were measured by Zipf and Gorman [21], James *et al* [22] and Ratliff *et al* [7]. Differential electronic excitation cross sections for N_2 have been also widely measured by several groups [16, 17, 23–26]. Itikawa [1, 27] gave detailed recommended values for the various collision cross sections for the ground state N_2 system.

Theoretically, studies of electronic excitation from the N_2 ground state are provided by several groups. Initially, Fliflet *et al* [28] and Mu-Tao and McKoy [29] presented distorted-wave calculations of differential and integral cross sections for excitation of the $A\ ^3\Sigma_u^+$, $B\ ^3\Pi_g$, $W\ ^3\Delta_u$, $w\ ^1\Delta_u$, $C\ ^3\Pi_u$, $E\ ^3\Sigma_g^+$, $b'\ ^1\Sigma_u^+$ and $c'\ ^1\Sigma_u^+$. Gillan *et al* [30, 31] used the R-matrix method to calculate integral excitation cross sections for the lowest seven ($A\ ^3\Sigma_u^+$, $B\ ^3\Pi_g$, $W\ ^3\Delta_u$, $B'\ ^3\Sigma_u^-$, $a\ ^1\Pi_g$, $a'\ ^1\Sigma_u^-$, $w\ ^1\Delta_u$)

states from the ground state. Then, Bettega *et al* [32] calculated the elastic integral and differential cross sections using Schwinger multichannel method with pseudopotentials. More recently, Tashiro and Morokuma [33] also employed the R-matrix method to calculate integral and differential excitation cross sections of the lowest eight ($A\ ^3\Sigma_u^+$, $B\ ^3\Pi_g$, $W\ ^3\Delta_u$, $B'\ ^3\Sigma_u^-$, $a\ ^1\Pi_g$, $a'\ ^1\Sigma_u^-$, $w\ ^1\Delta_u$ and $C\ ^3\Pi_u$) states. Meanwhile, Da Costa and Lima [8, 34] calculated integral and differential cross sections from ground state to $A\ ^3\Sigma_u^+$, $B\ ^3\Pi_g$, $W\ ^3\Delta_u$, $B'\ ^3\Sigma_u^-$, $a\ ^1\Pi_g$, $a'\ ^1\Sigma_u^-$ and $w\ ^1\Delta_u$ electronic states using the Schwinger multichannel method.

Up to now, there are few studies of electron impact on molecules in electronically excited state. Experimentally, such studies present difficulties relating to the separation of the different contributions arising from each excited state with sufficient accuracy, especially when these states are close in energy [35]. Even data on collisions with the simplest electronically excited hydrogen molecule comes exclusively from theory [36–38]. A handful of experimental and theoretical studies have been carried out on electrons collisions with excited oxygen molecule [39, 40]; there are also some studies on collisions with vibrationally excited moelcules [35]. For N_2 molecule, while electron collisions from vibrationally excited N_2 has been studies experimentally [41], the only data on electron scattering from excited electronic states are complex scattering potential calculations by Joshipura *et al* [9], who only considered the $A\ ^3\Sigma_u^+$ state.

The aim of the present work is to investigate electron-impact excitation of the eight lowest electronic states ($X\ ^1\Sigma_g^+$, $A\ ^3\Sigma_u^+$, $B\ ^3\Pi_g$, $W\ ^3\Delta_u$, $B'\ ^3\Sigma_u^-$, $a\ ^1\Pi_g$, $a'\ ^1\Sigma_u^-$, $w\ ^1\Delta_u$ and $C\ ^3\Pi_u$) from the ground state of N_2 in the low energy region using the fixed-nucleus R-matrix method. These results are compared to previous studies. To fill the existing gap in data for electronic transition between the excited states of N_2, we provide comprehensive data for processes starting from the two low-lying metastable$_=$ electronically excited states of N_2, the $A\ ^3\Sigma_u^+$ triplet state and the $a\ ^1\Pi_g$ singlet state and give a detailed analysis. The paper is organized as follows. In the next section, we give a brief review of the theoretical R-matrix method. Section 3 discusses the calculation details of the target states and scattering models. In section 4, we discussed the results for the studied collision processes. Section 5 presents our concluding remarks and perspectives.

2. Theoretical methods

The molecular fixed-nucleus R-matrix method provides a flexible way of calculating electron scattering data for a variety of electron collision processes. We offer a brief description of the R-matrix method since it has been extensively reviewed by Burke [42] and Tennyson [43]. In the framework of the R-matrix approach, configuration space is divided into an inner and an outer region by a sphere of radius $r = a$. In the inner region, the R-matrix calculation constructs and solves an energy-independent wave equation. The scattering electron interacts strongly with the target electrons through exchange, and correlation effects, and as such is accurately modelled using a configuration-interaction (CI) basis expansion for the

Table 1. Target energies in Hartree for the ground state and vertical excitation energies in eV for the first eight excited states of N_2 calculated based on cc-pVTZ and 6-311G** basis sets. These are compared with the R-matrix results of Gillan *et al* [32], Tashiro and Morokuma [34]; minimal orbital basis for single configuration interactions (MOBSCI) calculations from Da Costa and Lima [8, 35]; multireference singly and doubly excited configuration-interaction (MRSDCI) calculations from Pitarch-Ruiz *et al* [49]; as well as the experimental values fitted by Oddershede *et al* [50].

Target State	cc-pVTZ	6-311G**	R-matrix [31]	R-matrix [33]	MOBSCI	MRSDCI [48]	Expt. [49]
$X^1\Sigma_g^+$	-109.1137	-109.1027	-109.1215	—	—	—	—
$A^3\Sigma_u^+$	7.76	7.78	7.63	7.89	6.55 [34]	7.65	7.75
$B^3\Pi_g$	8.67	8.64	8.54	8.54	8.40 [8]	8.25	8.04
$W^3\Delta_u$	9.17	9.20	9.11	9.38	7.57 [34]	8.88	8.88
$B'^3\Sigma_u^-$	9.84	9.88	9.83	10.06	8.60 [34]	9.88	9.67
$a^1\Pi_g$	10.02	10.00	9.89	9.85	10.35 [8]	9.71	9.31
$a'^1\Sigma_u^-$	10.41	10.46	10.41	10.69	8.60 [34]	10.04	9.92
$w^1\Delta_u$	10.69	10.75	10.74	11.01	9.17 [34]	10.41	10.27
$C^3\Pi_u$	11.88	11.85	—	11.64	—	11.33	11.19

Table 2. Resonance positions and widths (in eV) for N_2 at the CC Level of approximation based on target models using cc-pVTZ and 6-311G** basis sets.

State	cc-pVTZ		6-311G**	
	Position	Width	Position	Width
$^2\Pi_g$	2.9027	0.6664	2.7423	0.5843
$^2\Sigma_g^-$	12.4106	1.3989	—	—
	12.5003	1.5921	12.2804	1.2789
$^2\Sigma_g^+$	—	—	12.3363	1.4804
$^2\Pi_u$	12.8709	1.6187	12.8458	2.3364
$^2\Sigma_u^+$	15.8129	2.0696	15.9401	1.6983
	15.9946	2.2682	15.8589	2.1587
$^2\Sigma_u^-$	—	—	15.8644	2.1790

total wavefunction in this region. In the outer region the scattering electron moves in the long-range multipole potential of the target molecule meaning that the scattering electron is influenced by the dipole and quadrupole moments of the target. The energy dependent scattering problem is solved entirely in the outer region in a relatively simple way.

In the inner region, calculations start by considering the *N*-electron target problem. Then the *N*-electron target plus scattering electron ($N + 1$) calculation gives a full description of the target interacting with the scattering electron within the R-matrix sphere. The wavefunction for the ($N + 1$) electron system is represented by a close-coupling (CC) expansion [43]:

$$\Psi_k^{N+1}\left(x_1, \ldots, x_{N+1}\right) = A \sum_{ij} a_{ijk}\varphi_i^N\left(x_1, \ldots, x_N\right) u_{ij}\left(x_{N+1}\right)$$
$$+ \sum_i b_{ik}\chi_i^{N+1}\left(x_1, \ldots, x_{N+1}\right),$$

where A is an anti-symmetrization operator which accounts for the exchange between the target electrons and the scattering electron, φ_i^N is the wavefunction of the *i*th target state, and χ_i^{N+1} are multicentre square-integrable (L^2) correlation functions. Moreover, u_{ij} are the continuum orbitals of the scattering electron, which is labelled by the target state index *i* as they depend on the symmetry of the particular target state, since the two must couple together to give the correct overall spatial and spin symmetry of the total wavefunction Ψ_k^{N+1}. The

variational coefficients for a_{ijk} and b_{ik} are determined by matrix diagonalization.

Studies of electron-impact electronic excitation and dissociation can be performed using the CC approximation. The CC scattering model includes a number of low-lying target states, depending upon the target model, which are represented by a CI expansion and includes hundreds of configurations in the second term. For this work, a CC model is employed to calculate resonance parameters and cross sections.

3. Target and scattering models

The calculations reported here are performed using the recently developed Quantemol electron collision (QEC) code [44] which runs both the MOLPRO package [45] and the new version of UK molecular R-matrix code UKRMol + [46]. The equilibrium geometry for N_2 molecule is with bond length $R = 1.104$ Å which is taken from NIST CCCBDB [47]. The N_2 molecule belongs to the $D_{\infty h}$ point group while we use the D_{2h} point group to solve the scattering problem since QEC [44] only provides Abelian point group symmetries.

Complete sets of molecular orbitals in the form of both occupied and virtual orbitals were obtained from complete active space self-consistent field calculations with Gaussian type orbital (GTO) cc-pVTZ and 6-311G** basis sets. The ground state ($X\ ^1\Sigma_g^+$) electronic configuration for the N_2 molecule is $1\sigma_g^2\ 1\sigma_u^2\ 2\sigma_g^2\ 2\sigma_u^2\ 1\pi_u^4\ 3\sigma_g^2$. Out of these 14 electrons, four core electrons of the target are frozen in the $1\sigma_g^2$ and $1\sigma_u^2$ molecular orbitals and the remaining electrons move freely in a complete active space which also includes the $1\pi_g$ and $3\sigma_u$ virtual orbitals. Between 136 and 192 configuration state functions are generated depending on the target symmetry. Nine target states are included in the CC expansion, namely the $X\ ^1\Sigma_g^+$, $A\ ^3\Sigma_u^+$, $B\ ^3\Pi_g$, $W\ ^3\Delta_u$, $B'\ ^3\Sigma_u^-$, $a\ ^1\Pi_g$, $a'\ ^1\Sigma_u^-$, $w\ ^1\Delta_u$ and $C\ ^3\Pi_u$ electronic states.

The nine target energies and vertical excitation energies are listed in table 1. To find the best target model for the description of the ground and excited states, we add a calculation based on 6-311G** basis set for comparison. The results based on cc-pVTZ and 6-311G** basis sets are slightly higher than those of and the R-matrix results of Gillan *et al* [31], the main
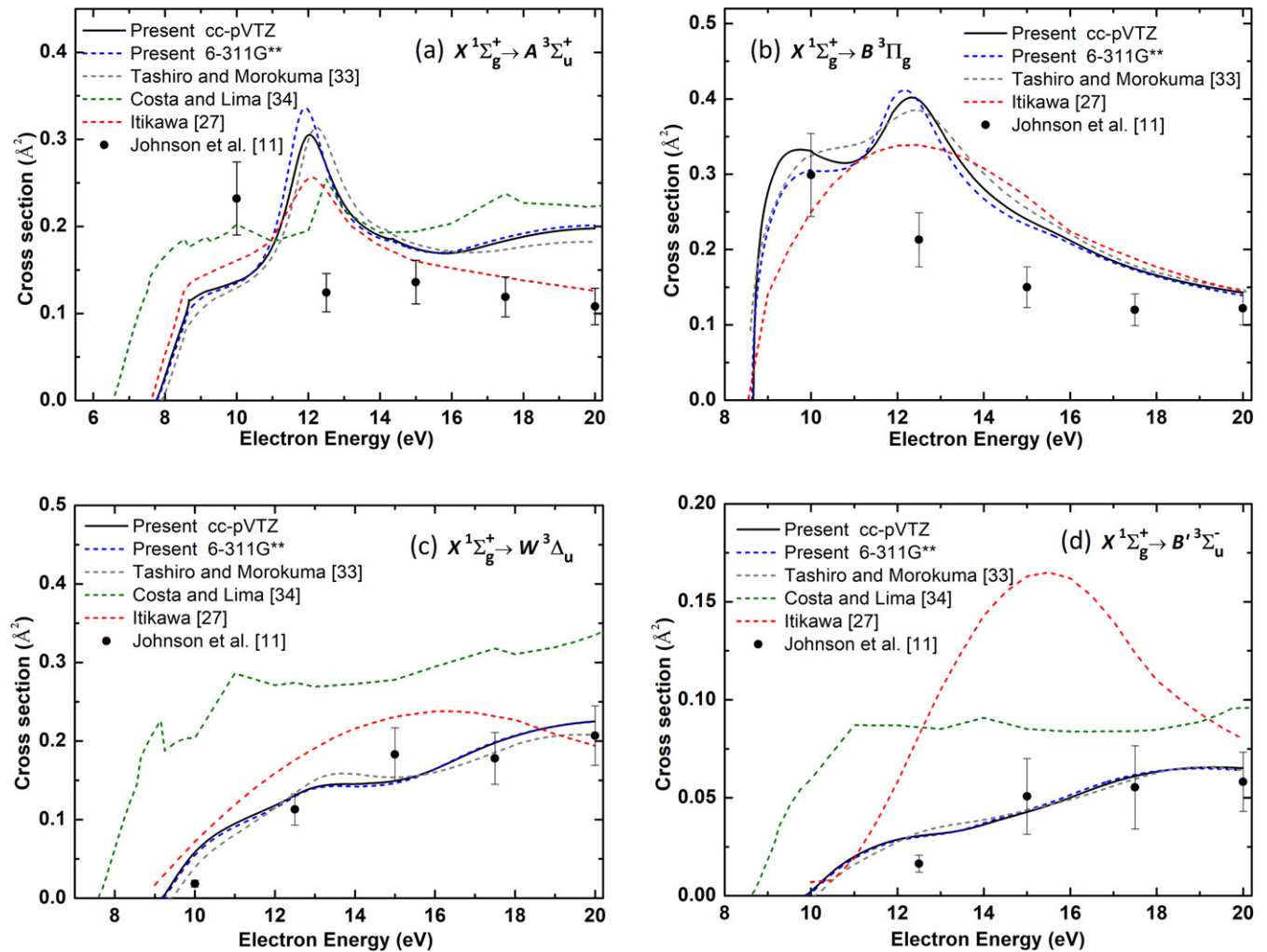
Figure 1. Excitation cross sections for N_2 from the $X\,^1\Sigma_g^+$ state to the (a) $A\,^3\Sigma_u^+$, (b) $B\,^3\Pi_g$, (c) $W\,^3\Delta_u$ and (d) $B'\,^3\Sigma_u^-$ excited states. Black solid line and blue dashed line respectively represent the present data from the target states with cc-pVTZ and 6-311G** basis sets. For comparison, we include the previous R-matrix calculations of Tashiro and Morokuma [33], Schwinger Multichannel results of Da Costa and Lima [34], the recommended data of Itikawa [27], as well as experimental results of Johnson *et al* [11].

difference is that they employed Slater type orbitals in their calculations to represent the target. Our calculations are closest in approach to the work of Tashiro and Morokuma [33] but our target basis includes extra diffuse and high *l* functions which leads to a somewhat improved representation of electronic excited states. Conversely, compared to the relatively crude minimal orbital basis single configuration interactions (MOBSCI) calculations reported by Da Costa and Lima [8, 34], the differences of up to 1.63 eV are found compared to our 6-311G** calculation for the $W\,^3\Delta_u$ state. The extensive multireference singly and doubly excited configuration-interaction (MRSDCI) electronic structure calculations of Pitarch-Ruiz *et al* [48], give a maximum deviation of 0.42 eV which is from $B\,^3\Pi_g$ state at cc-pVTZ level and $a'\,^1\Sigma_u^-$ state at 6-311G** level. On the whole, the present vertical excitation energies are slightly higher than the experimental results [49] which is to be expected as experimental values are adiabatic, that is allow for relaxation of the nuclei upon excitation.

Compared to the adiabatic experimental value [49], the maximum deviations of the present results with 0.69 and 0.70 eV respectively calculated from cc-pVTZ and 6-311G** basis sets are almost same, which are good considering the both levels of calculation. The first vertical excitation energies, 7.76 and 7.78 eV, from these two basis sets are almost the same as the fitted experimental value of 7.75 eV [49]. Therefore, the present N_2 target states are well modelled and reliable.

For the present scattering calculation, the inner region radius is taken to be 10 a_0 and the outer region R-matrices were propagated to 100 a_0. In order to represent the scattering electron, we included continuum orbitals which take the form of bond-centred GTOs fitted to Bessel functions with $l \leqslant 4$ [50]. Resonances were also detected and parameterised by fitting the eigenphase sum to a Breit–Wigner profile using the RESON [51] program within QEC [44]. The details of the resonance positions and widths based on cc-pVTZ and 6-311G** target models are given in table 2.
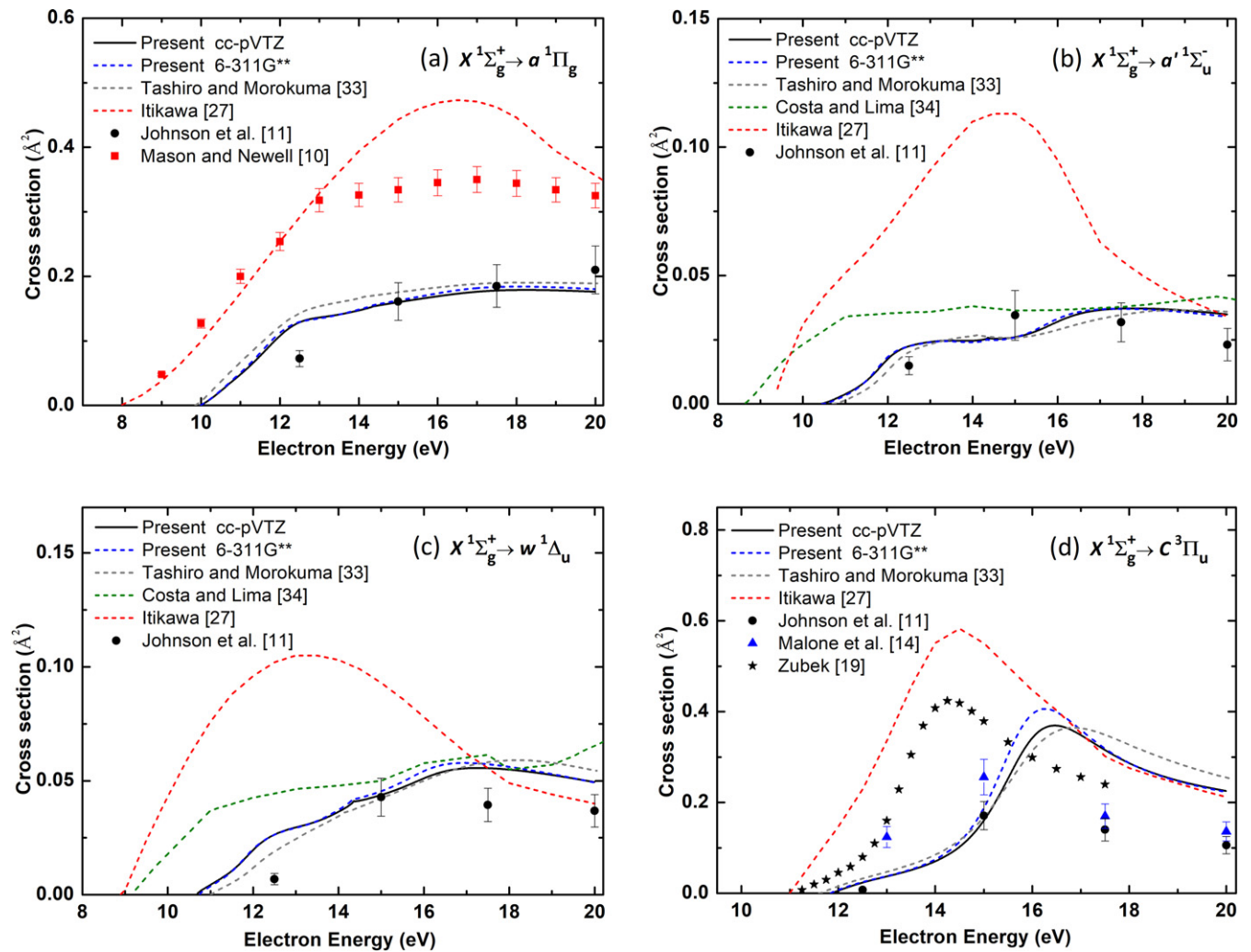
Figure 2. Excitation cross sections for N_2 from the $X\,^1\Sigma_g^+$ state to the (a) $a\,^1\Pi_g$, (b) $a'\,^1\Sigma_u^-$, (c) $w\,^1\Delta_u$ and (d) $C\,^3\Pi_u$ excited states. Black solid line and blue dashed line respectively represent the present data from the target states with cc-pVTZ and 6-311G** basis sets. For comparison, we not only include the reference values cited in figure 1, but also add the experimental data provided by Mason and Newell [10] in figure 2(a), as well as Malone *et al* [14] and Zubek [19] in figure 2(d).

4. Results and discussion

4.1. Ground state

In this section, elastic scattering and electronic excitation cross sections for electron impact on N_2 $X\,^1\Sigma_g^+$ ground state to the eight lowest excited states listed in table 1 are reported. The present results calculated based on cc-pVTZ and 6-311G** basis sets is compared with earlier measurements and theoretical data where available.

4.1.1. $X\,^1\Sigma_g^+ \to A\,^3\Sigma_g^+$. Figure 1 gives the electron impact excitation cross sections of the first four $A\,^3\Sigma_u^+$, $B\,^3\Pi_g$, $W\,^3\Delta_u$, and $B'\,^3\Sigma_u^-$ excited states from the $X\,^1\Sigma_g^+$ ground state. In figure 1(a), our excitation cross sections for $X\,^1\Sigma_g^+ \to A\,^3\Sigma_u^+$, which show a single peak, are in good agreement with the previous results of Tashiro and Morokuma [33] as well as Itikawa [27]. Moreover, the scaled shape of our calculation agrees very well with that of Da Costa and Lima [34] in the energy range from 12.5 to 15 eV. The present data are slightly

higher than the experimental results of Johnson *et al* [11] at the electron energy above 10 eV, and the present result is about twice the experimental value at around 20 eV. At higher incident energies, this is probably due to the absence of higher electronic states and ionisation channels in the R-matrix CC expansion which known to lead to overestimated cross-section, see Meltzer *et al* [52]. The present cross sections for excitation of the $A\,^3\Sigma_u^+$ state have a prominent resonance feature at around 12 eV, as seen in the previous R-matrix results of Tashiro and Morokuma [33] at 12.2 eV. Contributions to this peak structure in the present calculations come mainly from the $^2\Pi_u$ symmetry and partly from the $^2\Sigma_g$ symmetry as seen from the respective eigenphase sum given in table 2.

4.1.2. $X\,^1\Sigma_g^+ \to B\,^3\Pi_g$. As can be seen in figure 1(b), our excitation cross sections are no more than 0.42 Å^2 for the $B\,^3\Pi_g$ state which overall agree well with the results of Tashiro and Morokuma [33] and Itikawa [27], especially above 13 eV. The magnitude of our result is slightly larger than the experimental results of Johnson *et al* [11], and the maximum deviation
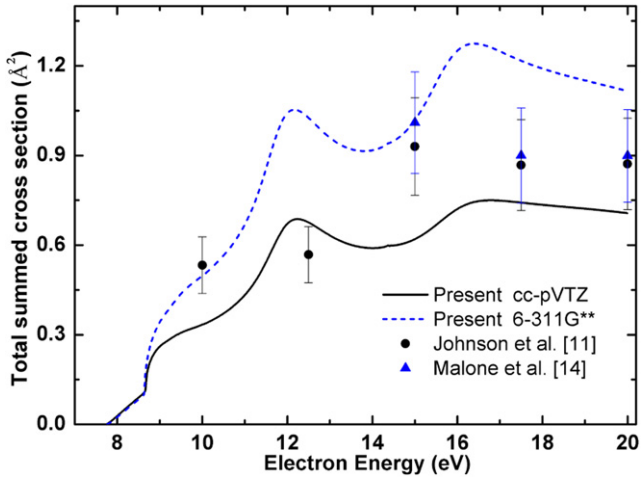
Figure 3. Summed cross sections for electron impact excitation of X $^1\Sigma_g^+$ to the $A\ ^3\Sigma_u^+$, $B\ ^3\Pi_g$, $W\ ^3\Delta_u$, $B'\ ^3\Sigma_u^-$, $a\ ^1\Pi_g$, $a'\ ^1\Sigma_u^-$, $w\ ^1\Delta_u$ and $C\ ^3\Pi_u$ states. Black solid line and blue dashed line respectively represent the present data from the target states with cc-pVTZ and 6-311G** basis sets; black solid circles, experimental results of Johnson *et al.* [11]; blue solid triangles, experimental results of Malone *et al.* [14].

Figure 4. Elastic scattering cross section for the N_2 $X\ ^1\Sigma_g^+$ ground state. This calculation: black solid line: cc-pVTZ basis set; blue dash line: 6-311G** basis set; gray dashed line: theoretical results of Tashiro and Morokuma [33]; red dashed line: the recommended values of Itikawa [27].

of cross section is from cc-pVTZ basis set calculation which is 0.19 Å^2 at incident electron energy of 12.5 eV. For the cc-pVTZ and 6-311G** basis sets, the calculated cross sections have a peak respectively at 12.3 eV and 12.1 eV, and we note that the peak position corresponds to the $^2\Sigma_g$ and $^2\Pi_u$ symmetry resonances. These findings are in agreement with the results of Tashiro and Morokuma [33].

4.1.3. $X\ ^1\Sigma_g^+ \rightarrow W\ ^3\Delta_u$ and $X\ ^1\Sigma_g^+ \rightarrow B'\ ^3\Sigma_u^-$. The excitation cross sections for the $W\ ^3\Delta_u$ and $B'\ ^3\Sigma_u^-$ states are shown in figures 1(c) and (d); the shape and magnitude of our results are almost the same as those from Tashiro and Morokuma [33]. Agreement with the experimental cross sections of Johnson *et al* [11] is also good in this case. Our scattering cross sections increase slowly with increasing incident electron energy up to 20 eV, which differs from the recommend data of Itikawa [27] which shows a broad peak at around 15 eV for both $W\ ^3\Delta_u$ and $B'\ ^3\Sigma_u$ excited states. Our cross sections for these two states are about half of the values provided by Da Costa and Lima [34] over the whole energy range. In addition, the excitation threshold energies in the present calculation are in good agreement with the theoretical values of Tashiro and Morokuma [33] and Itikawa [27] but a little higher than those of Da Costa and Lima [34]. The difference between ours and the calculations of Da Costa and Lima [34] may come from different number of target states considered in the scattering calculation.

4.1.4. $X\ ^1\Sigma_g^+ \rightarrow a\ ^1\Pi_g$. Figure 2 presents electronic excitation cross sections from the $X\ ^1\Sigma_g^+$ ground state to the four higher excited states we consider: $a\ ^1\Pi_g$, $a'\ ^1\Sigma_u^-$, $w\ ^1\Delta_u$ and $C\ ^3\Pi_u$. For excitation to the $a\ ^1\Pi_g$ state, shown in figure 2(a), our excitation cross section is almost identical to the experimental results of Johnson *et al* [11] except at the energy of 12.5 eV. It can be noted that the older measurements of Mason
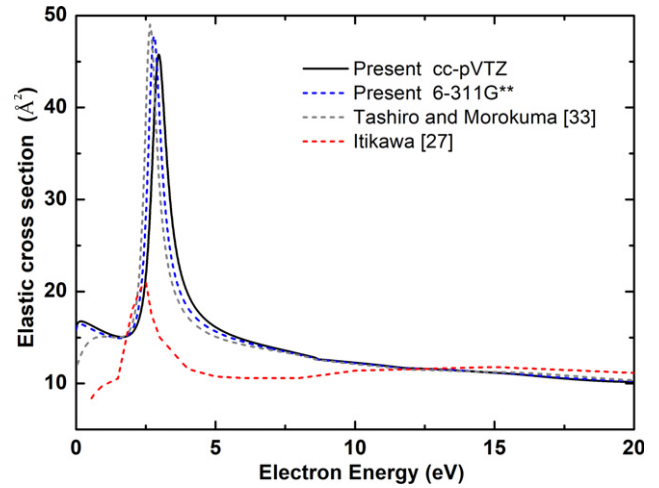
and Newell [10] gave cross sections about twice as large as our results at incident electron energy of 15–20 eV. It is possible that other metastable states were simultaneously detected since their detection technique lacked any suitable metastable state discrimination, which would lead to overestimated results. However, apart from the difference in magnitude, the shape of the present cross sections is similar to the results of Mason and Newell [10]. However, disagreements are observed between ours and the recommended values of Itikawa [27], especially at the energy ranging from 12 to 20 eV. Moreover, in common with the both experiments and the other theoretical studies, our results do not predict a peak in this region. It would appear that this recommendation of Itikawa [27] should be updated.

4.1.5. $X\ ^1\Sigma_g^+ \rightarrow a\ ^1\Sigma_u^-$ and $X\ ^1\Sigma_g^+ \rightarrow w\ ^1\Delta_u$. Figures 2(b) and (c) shows the results for the electronic excitation from the ground state to the $a'\ ^1\Sigma_u^-$ and $w\ ^1\Delta_u$ states. The excitation cross sections for both two excited states have similar shape and magnitude which is below 0.07 Å^2 for energies less than 20 eV, that is same as the $B'\ ^3\Sigma_u^-$ state. Our excitation cross sections for these two transitions are in very good agreement with the previous data of Tashiro and Morokuma [33] at all energy ranges and compare well with the data of Da Costa and Lima [34] at the energy above 15 eV. But the agreement with data recommended by Itikawa [27] is poor. The values of Itikawa [27] for the $a'\ ^1\Sigma_u^-$ and $w\ ^1\Delta_u$ states have a broad peak around 15 eV and 12.5 eV, respectively, which is different from our cross sections show a mild increase with energy in the range 15–20 eV. In practice, the absolute discrepancy is very small since the magnitudes of these cross sections are quite small. Moreover, the present results are roughly in agreement with the experimental values of Johnson *et al* [11]. Thus, we still believe that the R-matrix method calculations are reliable and again the recommendation should be updated.
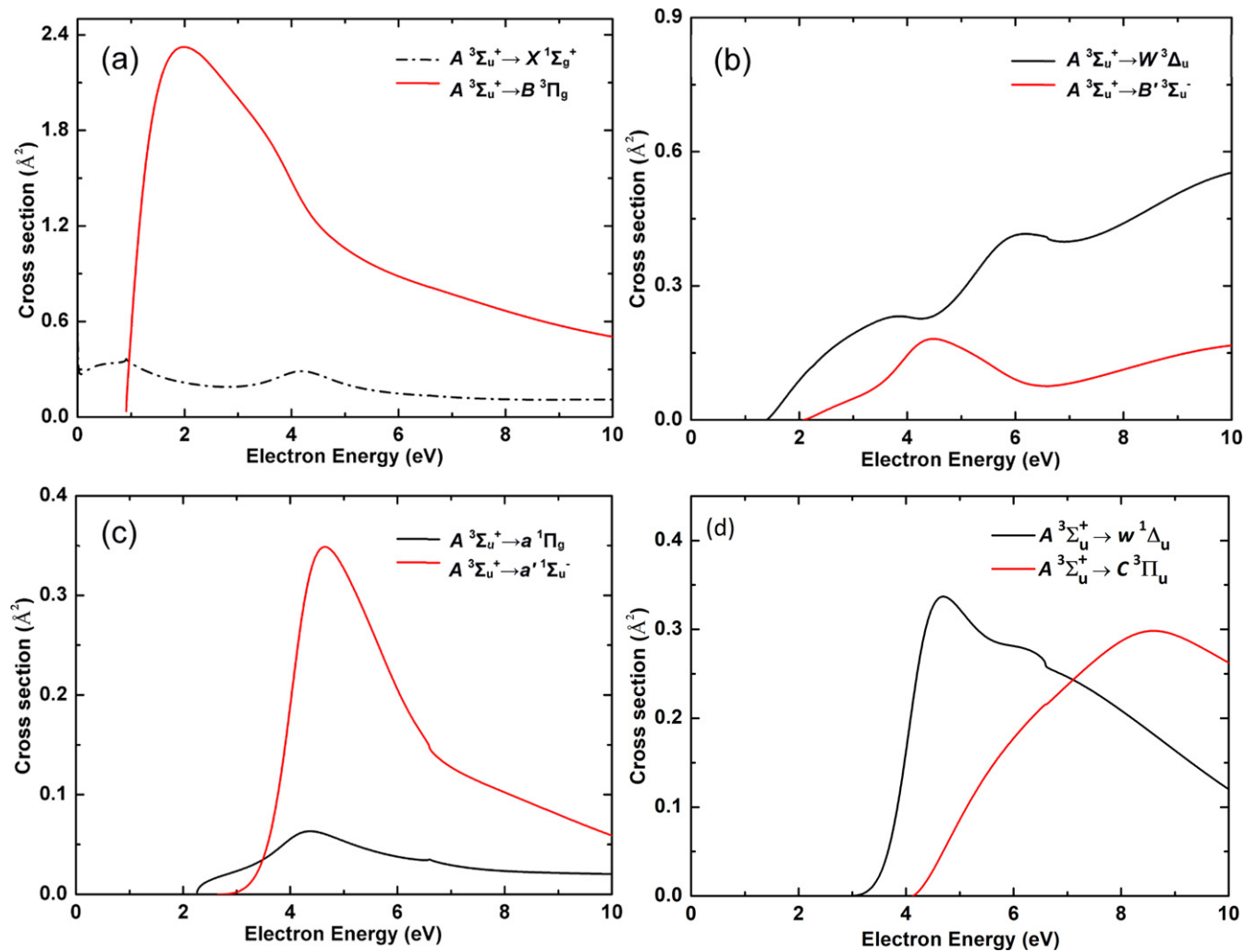
Figure 5. Electron impact excitation (solid line) and de-excitation (dot dash line) cross sections from the $A\,^3\Sigma_u^+$ excited state of N_2 to other low-lying states ($X\,^1\Sigma_g^+$, $B\,^3\Pi_g$, $W\,^3\Delta_u$, $B'\,^3\Sigma_u^-$, $a\,^1\Pi_g$, $a'\,^1\Sigma_u^-$, $w\,^1\Delta_u$ and $C\,^3\Pi_u$).

4.1.6. $X\,^1\Sigma_g^+ \to C\,^3\Pi_u$. The calculated cross sections for excitation of the $C\,^3\Pi_u$ state are illustrated in figure 2(d). This excitation is of particular importance since this transition gives rise to the UV emissions of the second positive band system ($C\,^3\Pi_u \to B\,^3\Pi_g$) [11]. We include the additional experimental data provided by Malone *et al* [14] and Zubek [19] for comparison. It shows that the present R-matrix calculations agree better with the measurements of Johnson *et al* [11] at 12.5 eV and 15 eV, but are closer to the more recently updated data of Malone *et al* [14] at 17.5 eV and 20 eV. Moreover, our electronic excitation cross sections display a peak respectively at around 16.4 and 16.2 eV, based on the calculations of cc-pVTZ and 6-311G** basis sets, which shows satisfactory agreement with the theoretical results of Tashiro and Morokuma [33], but the corresponding peaks are respectively located at 14.25 eV and 14.5 eV in the results of Zubek [19] and Itikawa [27]. The present calculation predicts $^2\Sigma_u$ resonance states in the energy range 15–16 eV but there are no resonances detected from 13 to 15 eV. The discrepancy in the cross-section peak might be related to the fixed-nucleus approximation employed

or the limitation of higher excited target states in the R-matrix model.

4.1.7. Total summed excitation and elastic scattering cross sections. Figure 3 compares the present total summed excitation cross sections with the existing measurements for the eight excited states studied. In order to understand the difference between the present R-matrix calculations and previous work, we also added the summed results based on the target model performed using a 6-311G** basis set. The total excitation cross sections calculated using the cc-pVTZ target basis is generally lower than those calculated at the 6-311G** level from threshold to 20 eV. The main difference between the two basis sets lies in the two peak positions, the electronic transitions for $X\,^1\Sigma_g^+ \to A\,^3\Sigma_u^+$, $B\,^3\Pi_g$ contribute to the the first peak at around 12 eV; the second position at about 16 eV is from electron excitation process of $X\,^1\Sigma_g^+ \to C\,^3\Pi_u$. On the whole, both of calculations agree well with the experimental data of Johnson *et al* [11] and Malone *et al* [14].

Figure 4 shows elastic scattering mainly contributes to the electron collision with N_2 ground state in the low-energy region, compared to the electron impact excitation. Both our
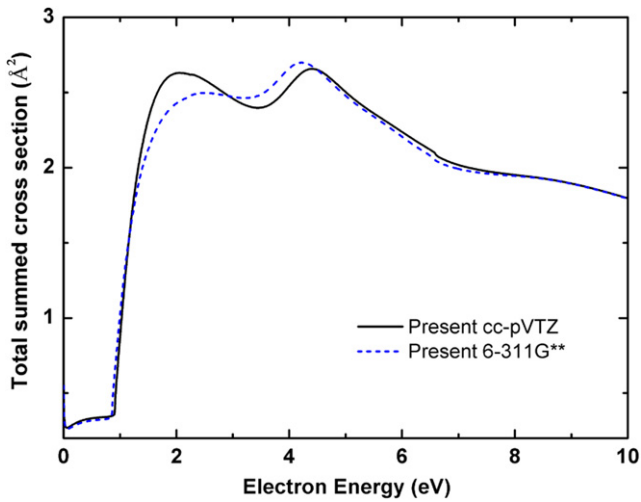
Figure 6. Summed cross sections for electron impact excitation from the $A\ ^3\Sigma_u^+$ state to the $X\ ^1\Sigma_g^+$, $B\ ^3\Pi_g$, $W\ ^3\Delta_u$, $B'\ ^3\Sigma_u^-$, $a\ ^1\Pi_g$, $a'\ ^1\Sigma_u^-$, $w\ ^1\Delta_u$ and $C\ ^3\Pi_u$ states. Black solid line and blue dashed line respectively represent the present data from the target states with cc-pVTZ and 6-311G** basis sets.
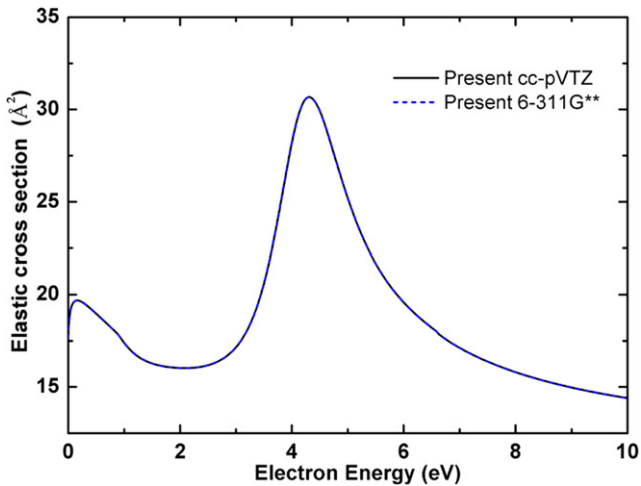

Figure 7. Elastic electron scattering cross section for the $N_2\ A\ ^3\Sigma_u^+$ excited state. Black solid line and blue dash line respectively represent the calculations from the target states with cc-pVTZ and 6-311G** basis sets.

elastic cross sections using cc-pVTZ and 6-311G** target models are roughly consistent with the previous results of Tashiro and Morokuma [33] over the whole energy range. Our elastic scattering cross sections have prominent peaks, which is a reflection of shape resonance state as is detected due to the $^2\Pi_g$ symmetry of an electronic state that corresponds to the temporary negative ion formation of N_2^-. This well-known $^2\Pi_g$ shape resonance has been observed many times [29, 31, 53]. The peak positions with 2.9 and 2.8 eV calculated from cc-pVTZ and 6-311G** basis sets are in agreement with earlier results of Tashiro and Morokuma [33] with 2.65 eV and Itikawa [27] with 2.5 eV. Additionally, the peak is more pronounced in our case than the recommended values of Itikawa [27] probably due to the neglect of nuclear motion in the present calculations.

In summary, the difference between our electronic excitation cross sections and the experimental results of Johnson *et al* [11] are very small; the agreement is especially good for electronic impact excitation of the $W\ ^3\Delta_u$, $B'\ ^3\Sigma_u^-$, $a\ ^1\Pi_g$, $a'\ ^1\Sigma_u^-$ and $w\ ^1\Delta_u$ states. The magnitude of excitation cross sections to the $A\ ^3\Sigma_u^+$, $B\ ^3\Pi_g$, $W\ ^3\Delta_u$, $a\ ^1\Pi_g$ and $C\ ^3\Pi_u$ states are larger than the corresponding excitation cross sections to the other three states. We can conclude that the R-matrix method can gives an accurate description of excitation cross sections in the low energy ranges. We therefore use this model for the calculations of electron scattering with N_2 excited states.

An important process in plasmas is electron impact dissociation. Usually this process goes via electron impact excitation of (dissociative) electronic states [54]. However, none of the 8 lowest excited states considered here are dissociative and thus this model would yield a very low value for the electron impact dissociation cross section; this is consistent with the recommendations of Itikawa [27] in the energy range we consider.

4.2. Metastable excited states

In this section we use the R-matrix method to study the excitation, de-excitation and elastic cross sections from the metastable $A\ ^3\Sigma_u^+$ triplet and $a\ ^1\Pi_g$ singlet states of N_2.

4.2.1. $A^3\Sigma_u^+$ electronic state. Figure 5 presents the de-excitation cross section for $A\ ^3\Sigma_u^+ \rightarrow X\ ^1\Sigma_g^+$ and excitation cross sections from the $A\ ^3\Sigma_u^+$ state to the $B\ ^3\Pi_g$, $W\ ^3\Delta_u$, $B'\ ^3\Sigma_u^-$, $a\ ^1\Pi_g$, $a'\ ^1\Sigma_u^-$, $w\ ^1\Delta_u$ and $C\ ^3\Pi_u$ seven states based on cc-pVTZ basis set. As the QEC calculations on N_2 only considers doublet spin symmetries, the quartet total spin symmetry which can connect the $A\ ^3\Sigma_u^+$ electronic state with other triplet states is not considered. Thus for triplet to triplet electronic transition processes, such as those from the $A\ ^3\Sigma_u^+$ to $B\ ^3\Pi_g$, $W\ ^3\Delta_u$, $B'\ ^3\Sigma_u^-$ and $C\ ^3\Pi_u$ as well as $A\ ^3\Sigma_u^+ \rightarrow A\ ^3\Sigma_u$ elastic scattering, we assume that the quartet contribution is simply twice that of the doublet on the grounds of spin degeneracy.

Figure 5(a) shows that the de-excitation cross sections of $A\ ^3\Sigma_u^+ \rightarrow X\ ^1\Sigma_g^+$ generally decreases with increase in the incident electron energy, except for the convex changes at the peaks position of 0.9 eV and 4.2 eV. The $A\ ^3\Sigma_u^+ \rightarrow B\ ^3\Pi_g$ electronic transition has a relatively large cross section with a peak at the energy around 2.0 eV. The excitation cross section of the $A\ ^3\Sigma_u^+ \rightarrow W\ ^3\Delta_u$, see figure 5(b), increases roughly with the increase of energy and reaches maximum value of 0.55 Å^2 at 10 eV. The electronic transitions of $A\ ^3\Sigma_u^+ \rightarrow a'$ $^1\Sigma_u^-$, see figure 5(c) and $A\ ^3\Sigma_u^+ \rightarrow w\ ^1\Delta_u$, see figure 5(d), are quite similar in shape and magnitude which are below 0.35 Å^2, and they both have a peak at around 4.7 eV which comes from the $^2\Sigma_g$ and $^2\Pi_u$ resonances. As for the $A\ ^3\Sigma_u^+ \rightarrow C\ ^3\Pi_u$ electronic transition in figure 5(d), the cross section is no more than 0.3 Å^2 and there is a broad peak at 8.6 eV. Finally, we note that there is a low probability for the electron impact excitation processes which go from the $A\ ^3\Sigma_u^+$ to the $B'\ ^3\Sigma_u^-$ and $a\ ^1\Pi_g$ metastable states; we note that both these processes are dipole forbidden.
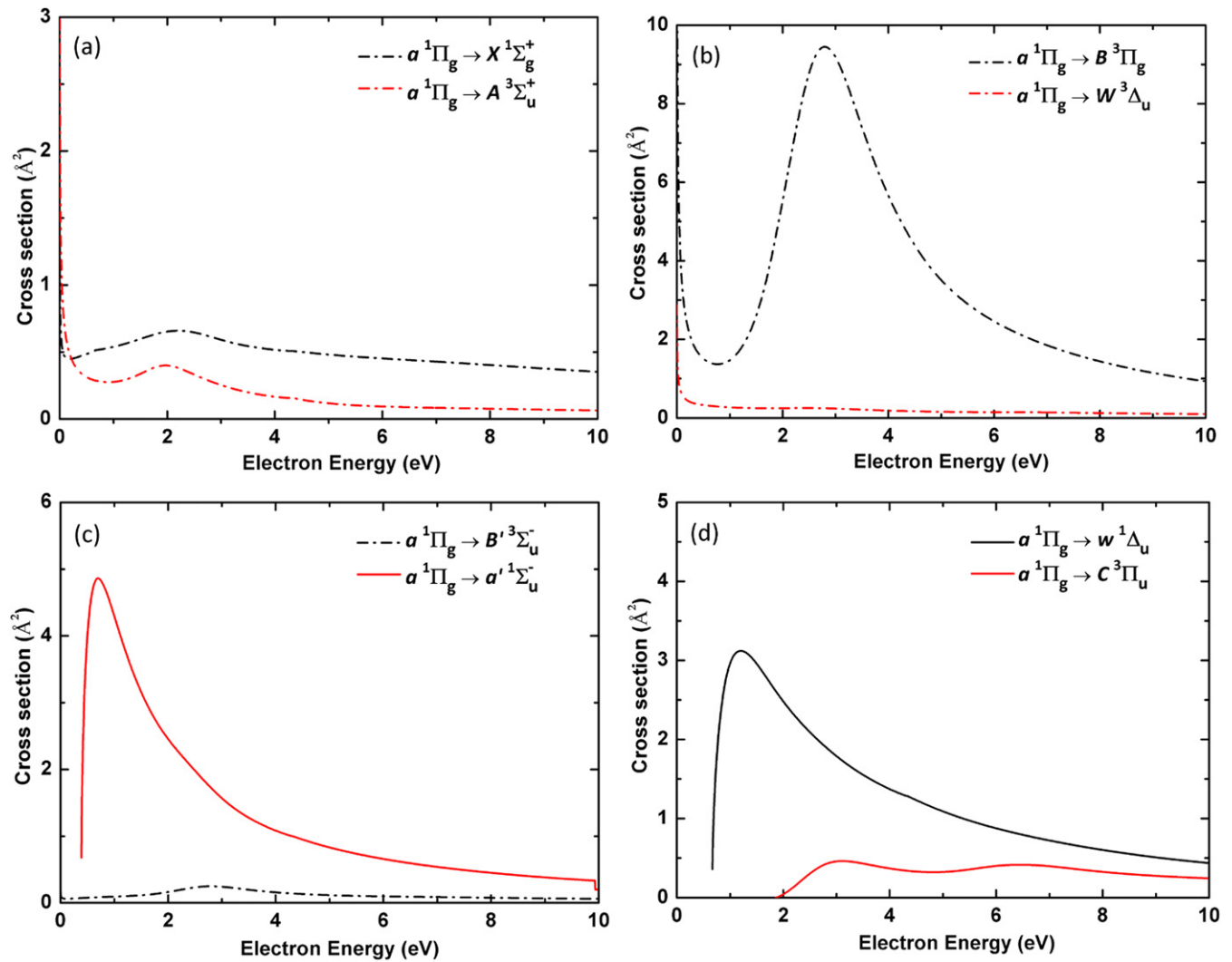
Figure 8. The individual electron impact excitation (solid line) and de-excitation (dot dash line) cross sections from the $a\,^1\Pi_g$ excited state of N_2 to eight low-lying states ($X\,^1\Sigma_g^+$, $A\,^3\Sigma_u^+$, $B\,^3\Pi_g$, $W\,^3\Delta_u$, $B'\,^3\Sigma_u^-$, $a'\,^1\Sigma_u^-$, $w\,^1\Delta_u$ and $C\,^3\Pi_u$).

The total cross sections shown in figure 6 are the sum of the individual cross sections of the eight electronic transitions for $A\,^3\Sigma_u^+ \to X\,^1\Sigma_g^+$, $B\,^3\Pi_g$, $W\,^3\Delta_u$, $B'\,^3\Sigma_u^-$, $a\,^1\Pi_g$, $a'\,^1\Sigma_u^-$, $w\,^1\Delta_u$ and $C\,^3\Pi_u$. As little is known about electron scattering from electronic excited states of N_2, we also considered a model based on use of 6-311G** target basis set for comparison. Joshipura *et al* [9] only consider compound excitation cross sections for collisions occurring at higher energies so a comparison with their results is not possible. Our summed results below 1.2 eV are mainly due to the contribution of the $A\,^3\Sigma_u^+ \to X\,^1\Sigma_g^+$ de-excitation process, but increase rapidly in the scattering energy between 1.2 eV to 2.0 eV. It shows that the electronic transitions cross sections from the $A\,^3\Sigma_u^+$ excited state are largest in the energy range from 2.0 eV to 10 eV. Figure 7 shows elastic scattering cross sections for the $A\,^3\Sigma_u^+$ state. There is a very pronounced resonance peak at around 4.2 eV, which mainly comes from the $^2\Sigma_g$ and $^2\Pi_u$ symmetries. And the peak height is about three fifths of those of elastic scattering of $X\,^1\Sigma_g^+ \to X\,^1\Sigma_g^+$ in figure 4. It also can be concluded that the present excitation, de-excitation and elastic

cross sections calculated using target models at cc-pVTZ and 6-311G** level give almost the same results.

4.2.2. $a\,^1\Pi_g$ electronic state. Figure 8 presents excitation and de-excitation cross sections from the $a\,^1\Pi_g$ excited state to all the states listed in table 1 based on cc-pVTZ basis set. In general, the de-excitation cross sections, $a\,^1\Pi_g \to X\,^1\Sigma_g^+$, $A\,^3\Sigma_u^+$ and $W\,^3\Delta_u$ shown in figures 8(a) and (b) decrease with increasing incident electron energy. However, there is an exception for the $a\,^1\Pi_g \to B\,^3\Pi_g$ de-excitation process shown in figure 8(b) which has a very prominent peak at 2.8 eV. The dominant component in this cross section is the $^2\Pi_u$ symmetry. Moreover, the magnitude of the $a\,^1\Pi_g \to B\,^3\Pi_g$ cross section at its peak position is more than ten times larger than those of the other de-excitation processes. Therefore, we believe the $a\,^1\Pi_g \to B\,^3\Pi_g$ electron transition for N_2 is likely to play an important role in atmospheric processes and plasma emissions; in particular, the $B\,^3\Pi_g$ state plays a key role in the so-called first positive system of the N_2 electronic transitions [55].
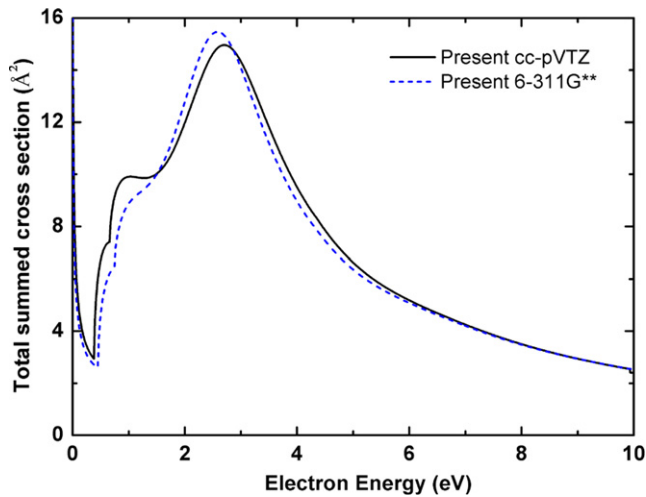
J. Phys. B: At. Mol. Opt. Phys. **54** (2021) 115203

H Su *et al*

Figure 9. Summed cross sections for electron impact electronic (de-)excitation of the a $^1\Pi_g$ state to the X $^1\Sigma_g^+$, A $^3\Sigma_u^+$, B $^3\Pi_g$, W $^3\Delta_u$, B' $^3\Sigma_u^-$, a' $^1\Sigma_u^-$, w $^1\Delta_u$ and C $^3\Pi_u$ states. Black solid line and blue dashed line respectively represent the present data from the target states with cc-pVTZ and 6-311G** basis sets.

Figure 10. Elastic electron scattering cross section for the N$_2$ a $^1\Pi_g$ excited state. The black solid line and blue dash line respectively represent the calculations from the target states with cc-pVTZ and 6-311G** basis sets.

The transitions a $^1\Pi_g \to a'$ $^1\Sigma_u^-$ and a $^1\Pi_g \to w$ $^1\Delta_u$ in figures 8(c) and (d) are the first two electronic excitation processes for electron impact of the a $^1\Pi_g$ state. They are both dipole allowed and have similar shapes, while the former is larger in the energy range of 0–2.5 eV. The remaining two dipole forbidden electronic transitions a $^1\Pi_g \to B'$ $^3\Sigma_u^-$ and a $^1\Pi_g \to C$ $^3\Pi_u$ have a much smaller cross section, which means that these processes contribute to the total cross sections are quite small.

Figure 9 gives the total summed cross sections of electron transitions from the a $^1\Pi_g$ state to the X $^1\Sigma_g^+$, A $^3\Sigma_u^+$, B $^3\Pi_g$, W $^3\Delta_u$, B' $^3\Sigma_u^-$, a' $^1\Sigma_u^-$, w $^1\Delta_u$ and C $^3\Pi_u$ states. And figure 10 gives the corresponding elastic scattering cross sections. The figure shows that both elastic and total summed cross sections have a peak at around 2.6 eV which coincides with the position of the $^2\Sigma_g$ symmetry resonance.

The summed cross sections based on target models using cc-pVTZ and 6-311G** basis sets give almost the same results for all energies. The peak height of the summed cross section are about six times larger than those of electrons colliding with the A $^3\Sigma_u^+$ state in figure 6 but is about ten times larger than those results from the ground X $^1\Sigma_g^+$ state in figure 3. This is because the large a $^1\Pi_g \to B$ $^3\Pi_g$ cross section raises the whole total summed cross section. In figure 10, the cross sections for the 6-311G** target representation are larger than those of cc-pVTZ target below the peak position. Furthermore, there is another peak at 0.2 eV for the calculation with 6-311G** basis set. These differences are caused by the difference resonance structures given by the two basis sets in the region, see the 12 eV resonances given in table 2. The peak heights of the elastic scattering for both target basis sets are a bit higher than those of the A $^3\Sigma_u^+$ metastable state in figure 7.
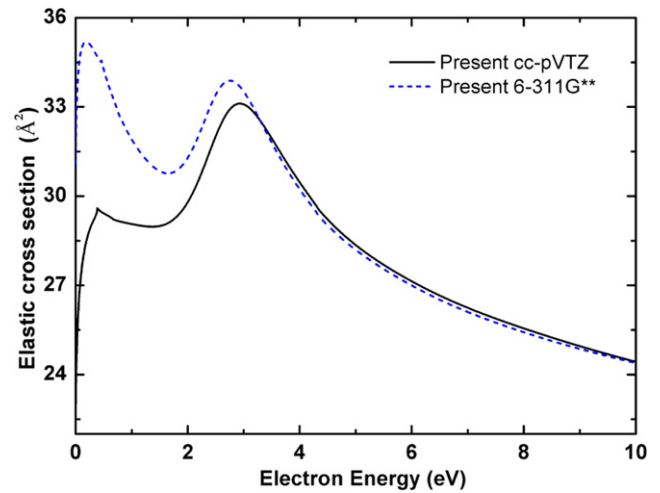
5. Conclusions

We investigate the electron impact scattering cross sections for molecular nitrogen from its ground X $^1\Sigma_g^+$ state as well as the excited A $^3\Sigma_u^+$ and a $^1\Pi_g$ metastable states to the nine electronic states, X $^1\Sigma_g^+$, A $^3\Sigma_u^+$, B $^3\Pi_g$, W $^3\Delta_u$, B' $^3\Sigma_u^-$, a $^1\Pi_g$, a' $^1\Sigma_u^-$, w $^1\Delta_u$ and C $^3\Pi_u$, using the R-matrix method. Spreadsheets containing our cross sections are provided as supplementary data (https://stacks.iop.org/JPB/00/000000/mmedia) to this paper. The vertical excitation energies are in good agreement with the previous reference values. For the X $^1\Sigma_g^+$ N$_2$ ground state, the present elastic and electron excitation scattering cross sections are in good agreement with the available literature results. It can be concluded that the R-matrix calculations perform well for electron collisions with ground molecular N$_2$ in the low-energy (below 20 eV) region.

Cross sections for electron impact (de-)excitation from the A $^3\Sigma_u^+$ and a $^1\Pi_g$ metastable states of N$_2$ are studied by the R-matrix method for the first time. The $^2\Sigma_g$ and $^2\Pi_u$ symmetries make the dominant contribution to resonance peak of the elastic and total summed cross sections. The present resonance analysis should also assist us in understanding the dissociative electron attachment and other resonance driven phenomena in N$_2$. So far theoretical studies have only considered the effect from the well-know, low-lying $^2\Pi_g$ shape resonance [53], however the higher lying resonances may also play an important role.

The magnitude of the total summed cross section for electron scattering from a $^1\Pi_g$ excited state is larger than those of X $^1\Sigma_g^+$ ground state by an order of magnitude. Additionally, we conclude that the de-excitation cross sections generally show a downward trend with the increase of incident electron

J. Phys. B: At. Mol. Opt. Phys. **54** (2021) 115203

H Su *et al*

energy, which is different from the elastic and electronic excitation scattering cross sections. However, there is a prominent resonance peak originating from $^2\Pi_u$ symmetry at 2.8 eV for the de-excitation process of the $a\ ^1\Pi_g \rightarrow B\ ^3\Pi_g$, which is the major contributor to the total cross sections from the excited $a\ ^1\Pi_g$ state. The present cross sections have potentially significant implications on our understanding of UV emissions in the atmospheres of Earth and Titan, as well as nitrogen plasmas.

Data availability statement

All data that support the findings of this study are included within the article and the supplementary files.

Acknowledgments

ORCID iDs

Hong Zhang https://orcid.org/0000-0003-3098-7988
Jonathan Tennyson https://orcid.org/0000-0002-4994-5238

REFERENCES

[1] Itikawa Y, Hayashi M, Ichimura A, Onda K, Sakimoto K, Takayanagi K, Nakamura M, Nishimura H and Takayanagi T 1986 *J. Phys. Chem. Ref. Data* **15** 985–1010
[2] Sun W, Morrison M A, Isaacs W A, Trail W K, Alle D T, Gulley R J, Brennan M J and Buckman S J 1995 *Phys. Rev.* A **52** 1229–56
[3] Tabata T, Shirai T, Sataka M and Kubo H 2006 *At. Data Nucl. Data Tables* **92** 375–406
[4] Vinodkumar M, Limbachiya C and Barot M 2012 *Mol. Phys.* **110** 3015–22
[5] Little D A, Chakrabarti K, Mezei J Z, Schneider I F and Tennyson J 2014 *Phys. Rev.* A **90** 052705
[6] Nijdam S, Teunissen J and Ebert U 2020 *Plasma Sources Sci. Technol.* **29** 103001
[7] Ratliff J M, James G K, Trajmar S, Ajello J M and Shemansky D E 1991 *J. Geophys. Res.* **96** 17559–61
[8] Da Costa R F and Lima M A P 2006 *Int. J. Quantum Chem.* **106** 2664–76
[9] Joshipura K N, Gangopadhyay S S, Kothari H N and Shelat F A 2009 *Phys. Lett.* A **373** 2876–81
[10] Mason N J and Newell W R 1987 *J. Phys. B: At. Mol. Phys.* **20** 3913–21
[11] Johnson P V, Malone C P, Kanik I, Tran K and Khakoo M A 2005 *J. Geophys. Res.* **110** A11311
[12] Blaauw H J, De Heer F J, Wagenaar R W and Barends D H 1977 *J. Phys. B: At. Mol. Phys.* **10** L299–303
[13] Muse J, Silva H, Lopes M C A and Khakoo M A 2008 *J. Phys. B: At. Mol. Opt. Phys.* **41** 095203
[14] Malone C P, Johnson P V, Young J A, Liu X, Ajdari B, Khakoo M A and Kanik I 2009 *J. Phys. B: At. Mol. Opt. Phys.* **42** 225202

[15] Campbell L, Brunger M J, Nolan A M, Kelly L J, Wedding A B, Harrison J, Teubner P J O, Cartwright D C and McLaughlin B 2001 *J. Phys. B: At. Mol. Opt. Phys.* **34** 1185–99
[16] Malone C P, Johnson P V, Liu X, Ajdari B, Kanik I and Khakoo M A 2012 *Phys. Rev.* A **85** 062704
[17] Finn T G and Doering J P 1976 *J. Chem. Phys.* **64** 4490–4
[18] Ajello J M and Shemansky D E 1985 *J. Geophys. Res.* **90** 9845–61
[19] Zubek M 1994 *J. Phys. B: At. Mol. Opt. Phys.* **27** 573–81
[20] Meng X, Wu B, Gao X-F, Xie J-C, Li H, Yu Y, Zhao D-F and Tian S X 2020 *J. Chem. Phys.* **153** 024301
[21] Zipf E C and Gorman M R 1980 *J. Chem. Phys.* **73** 813–9
[22] James G K, Ajello J M, Franklin B and Shemansky D E 1990 *J. Phys. B: At. Mol. Opt. Phys.* **23** 2055–81
[23] Khakoo M A, Malone C P, Johnson P V, Lewis B R, Laher R, Wang S, Swaminathan V, Nuyujukian D and Kanik I 2008 *Phys. Rev.* A **77** 012704
[24] Malone C P, Johnson P V, Kanik I, Ajdari B and Khakoo M A 2009 *Phys. Rev.* **79** 032704
[25] Malone C P, Johnson P V, Kanik I, Ajdari B, Rahman S S, Bata S S, Emigh A and Khakoo M A 2009 *Phys. Rev.* A **79** 032705
[26] Kato H, Suzuki D, Ohkawa M, Hoshino M, Tanaka H, Campbell L and Brunger M J 2010 *Phys. Rev.* A **81** 042717
[27] Itikawa Y 2006 *J. Phys. Chem. Ref. Data* **35** 31–53
[28] Fliflet A W, McKoy V and Rescigno T N 1979 *J. Phys. B: At. Mol. Phys.* **12** 3281–93
[29] Mu-Tao L and Mckoy V 1983 *Phys. Rev.* A **28** 697–705
[30] Gillan C J, Noble C J and Burke P G 1990 *J. Phys. B: At. Mol. Opt. Phys.* **23** L407–13
[31] Gillan C J, Tennyson J, McLaughlin B M and Burke P G 1996 *J. Phys. B: At. Mol. Opt. Phys.* **29** 1531–47
[32] Bettega M H F, Lima M A P and Ferreira L G 1998 *J. Phys. B: At. Mol. Opt. Phys.* **31** 2091–9
[33] Tashiro M and Morokuma K 2007 *Phys. Rev.* A **75** 012720
[34] Da Costa R F and Lima M A P 2007 *Phys. Rev.* A **75** 022705
[35] Brunger M J and Buckman S J 2002 *Phys. Rep.* **357** 215–458
[36] Sartori C S, da Paixão F J and Lima M A P 1997 *Phys. Rev.* A **55** 3243–6
[37] Sartori C S, da Paixão F J and Lima M A P 1998 *Phys. Rev.* A **58** 2857–63
[38] Meltzer T and Tennyson J 2020 *J. Phys. B: At. Mol. Opt. Phys.* **53** 245203
[39] Hall R I and Trajmar S 1975 *J. Phys. B: At. Mol. Phys.* **8** L293
[40] Tashiro M, Morokuma K and Tennyson J 2006 *Phys. Rev.* A **73** 052707
[41] Burrow P D and Davidovits P 1968 *Phys. Rev. Lett.* **21** 1789–91
[42] Burke P G 2011 *R-matrix Theory of Atomic Collisions* (*Springer Series on Atomic, Optical and Plasma Physics* vol 61) (Berlin: Springer)
[43] Tennyson J 2010 *Phys. Rep.* **491** 29–76
[44] Cooper B *et al* 2019 *Atoms* **7** 97
[45] Werner H-J *et al* 2009 *MOLPRO, Version 2009.1, A Package of Ab initio Programs* see http://www.molpro.net
[46] Mašín Z, Benda J, Gorfinkiel J D, Harvey A G and Tennyson J 2020 *Comput. Phys. Commun.* **249** 107092
[47] Johnson III R D 2020 http://cccbdb.nist.gov
[48] Pitarch-Ruiz J, Sánchez-Marín J, Nebot-Gil I and Amor N B 1998 *Chem. Phys. Lett.* **291** 407–13
[49] Oddershede J, Grüner N E and Diercksen G H F 1985 *Chem. Phys.* **97** 303–10
[50] Faure A, Gorfinkiel J D, Morgan L A and Tennyson J 2002 *Comput. Phys. Commun.* **144** 224–41
[51] Tennyson J and Noble C J 1984 *Comput. Phys. Commun.* **33** 421–4

J. Phys. B: At. Mol. Opt. Phys. **54** (2021) 115203

H Su *et al*

[52] Meltzer T, Tennyson J, Mašín Z, Zammit M C, Scarlett L H, Fursa D V and Bray I 2020 *J. Phys. B: At. Mol. Opt. Phys.* **53** 145204

[53] Laporta V, Little D A, Celiberto R and Tennyson J 2014 *Plasma Sources Sci. Technol.* **23** 065002

[54] Stibbe D T and Tennyson J 1998 *New J. Phys.* **1** 2

[55] Western C M, Carter-Blatchford L, Crozet P, Ross A J, Morville J and Tokaryk D W 2018 *J. Quant. Spectrosc. Radiat. Transfer* **219** 127–41